

OBSERVATIONS OF THE ELECTRICAL ASTHENOSPHERE BENEATH SCANDINAVIA

ALAN G. JONES *

Institut für Geophysik der Westfälischen Wilhelms-Universität, Corrensstrasse 24, D-4400 Münster (Federal Republic of Germany)

(Final version received December 29, 1981)

ABSTRACT

Jones, A.G., 1982. Observations of the electrical asthenosphere beneath Scandinavia. In: E.S. Husebye (Editor), *The Structure of the Lithosphere–Asthenosphere in Europe and the North Atlantic*. *Tectonophysics*, 90: 37–55.

The recent recognition that long period (i.e., of the order of hours) electromagnetic induction studies could play a major role in the detection of the asthenosphere has led to much interest amongst the geophysical and geological communities of the geomagnetic response functions derived for differing tectonic environments. Experiments carried out on the ocean bottom have met with considerable success in delineating the “electrical asthenosphere”, i.e., a local maximum in electrical conductivity (minimum in electrical resistivity) in the upper mantle.

In this paper, observations of the time-varying magnetic field recorded in three regions of Scandinavia, northern Sweden (Kiruna—KIR), northern Finland/northeastern Norway (Kevo—KEV), and southern Finland (Sauvamaki—SAU), are analysed in order to obtain estimates of the inductive response function, $C(\omega)$, for each region. The estimated response functions are compared with one from the centre of the East European Platform (EEP), and it is shown that the induced eddy currents, at periods of the order of 10^3 – 10^4 s, in the three regions flow much closer to the surface than under the platform centre. Specifically, at a period of ~ 3000 s, these currents are flowing at depths of the order of: KEV—120 km; KIR—180 km; SAU—210 km; EEP—280 km; implying that the transition to a conducting zone, of $\sigma \approx 0.2$ S/m, occurs at around these depths. One-dimensional inversion of \hat{C}_{KEV} and \hat{C}_{KIR} shows that there must exist a good conducting zone, of $\sigma = 0.1$ – 1.0 S/m, under each of the two regions, of 40 km minimum thickness, at depths of: KEV 105–115 km; KIR 160–185 km. This is to be contrasted with EEP, where the ρ – d profile displays a monotonically decreasing resistivity with depth, reaching $\sigma \sim 0.1$ S/m at > 300 km.

Finally, a possible temperature range for the asthenosphere, consistent with the deduced conductivity, is discussed. It is shown that, at present, there is insufficient knowledge of the conditions (water content, melt fraction, etc.) likely to prevail in the asthenosphere to narrow down the probable range of 900° – 1500°C .

* Present address: Geophysics Laboratory, Department of Physics, Toronto University, 60 St. George Street, Toronto, Ont. M5S 1A7 (Canada)

INTRODUCTION

Many geophysical methods exist for studying the structure of the Earth on global, regional, and local scales. All invoke measurement of one or more physical parameter(s), either time variant or invariant, and then attempt to invert the observed response to derive a model structure which is both unique and representative of the true Earth. Of those techniques that are applied for regional studies, geomagnetic induction methods offer one of the most powerful approaches for deducing temperature profiles within the Earth because, of all lithological parameters that are temperature dependent, conductivity is the most sensitive to thermal variation. However, the primary aim of the majority of induction studies is to derive a (unique) conductivity model that is consistent with the observed data. When this aim is achieved, a possible geothermal profile beneath the recording site *may* be derived from knowledge of the laboratory behaviour of the electrical conductivity of rocks, of which the mantle is most likely to be constituted, at high temperatures and pressures.

Geomagnetic induction studies utilise the time variations of the natural external magnetic field variations as the energy source, and penetration of these variations into the Earth is assured because of the skin-depth phenomenon of electro-magnetic fields. These variations diffuse into the Earth and induce electric currents by the elementary Faraday–Henry law, and the induced electric currents in turn induce secondary magnetic fields according to the Biot–Savart law. An observer on the surface of the Earth measures either (i) the three components of the time-varying magnetic field at one (single station Geomagnetic Deep Sounding) or synoptically at many (multi-station Geomagnetic Deep Sounding and Horizontal Spatial Gradient) locations, or (ii) the variations at one location of the two horizontal components of both the electric (telluric) and magnetic time-varying fields (Magneto-Telluric). The Geomagnetic Deep Sounding (GDS) method is usually employed to delineate anomalous conductivity structures by mapping current concentrations (see reviews by Gough, 1973a, b; Frazer, 1974; Lilley, 1975). For a one-dimensional (1D) earth, the Horizontal Spatial Gradient (HSG) and the Magneto-Telluric (MT) methods are more powerful in that direct estimates of the electrical conductivity distribution with depth can be attained. (The MT method can also be applied to 2D or 3D earth structures.)

Of great interest amongst the geomagnetic induction community at present is the detection, identification and location of the electrical asthenosphere—the ELAS Project (for *e*lectrical *a*sthenosphere). Certainly, a much clearer picture of the global variation of the maximum in electrical conductivity that occurs in the upper 200 km of the mantle, which is identified as the “electrical asthenosphere”, would lead to a greater understanding of plate tectonics and its orogenic implications.

As well as inferring a geothermal profile for the lithosphere and asthenosphere, geomagnetic induction studies may also indicate a possible viscosity profile. This is

because both electrical conductivity and effective viscosity of condensed non-metallic phases are thermally activated atomic processes, thus it is hardly surprising that there appears to be a correlation between them, i.e., minima in viscosity profiles are approximately at the same depth as maxima in conductivity profiles (Tozer, 1981).

In this work, HSG data from three regions in Scandinavia (northern Sweden; northern Finland/northeastern Norway; southern Finland) will be analysed, and the respective Inductive Response Functions ($C(\omega)$) for those regions will be derived. The response functions from each region will be examined for validity, and ρ - d (resistivity–depth) profiles of theoretical models consistent with two of them (\hat{C}_{KIR} and \hat{C}_{KEV}) will be presented. The response functions from the three locations require a transition to a high conducting zone, of $\sigma = 0.1$ – 1.0 S/m, within the top 100–250 km of the upper mantle. These observations will be compared with the data for the East European Platform, as published by Vanyan et al. (1977), and the conclusion drawn that the depth to the top of the electrical asthenosphere increases with increasing distance toward the centre of the continent. Finally, inferences about the possible temperature within the asthenosphere, from its deduced electrical conductivity, will be discussed.

DATA ANALYSIS, RESPONSE FUNCTIONS DERIVED AND VALIDITY

Data

The data that were analysed and interpreted in this study were recorded by the Münster University IMS (International Magnetospheric Study) magnetometer array (Küppers et al., 1979) of 36 modified Gough–Reitzel variometers (Gough and Reitzel, 1967; Küppers and Post, 1981), and the Braunschweig University chain of six Fluxgate magnetometers (Maurer and Theile, 1978). The locations of the instruments are illustrated in Fig. 1, together with the Cartesian co-ordinate system employed (introduced in Küppers et al. (1979) and named the “Kiruna system”). Three groups of stations will be considered here, situated in northern Sweden, northern Finland/northeastern Norway, and the southern part of central Finland, and are, respectively,

(i) the *Kiruna (KIR)* group of ten stations: EVE–RIJ–KVI–SRV–ROS–KIR–NAT–MIE–MUO–PEL,

(ii) the *Kevo (KEV)* group of nine stations: MAT–MIE–MUO–KUN–KEV–IVA–MAR–VAD–SKO,

(iii) the *Sauwamaki (SAU)* group of three stations: HOP–JOK–SAU.

All magnetometers in the three groups, with the one exception of HOP, were operating with a temporal resolution of 10 s, and a magnetic field variation resolution of 2 nT for the modified Gough–Reitzel’s (Küppers et al., 1979) and 0.5 nT for the Fluxgate’s (Maurer and Theile, 1978).

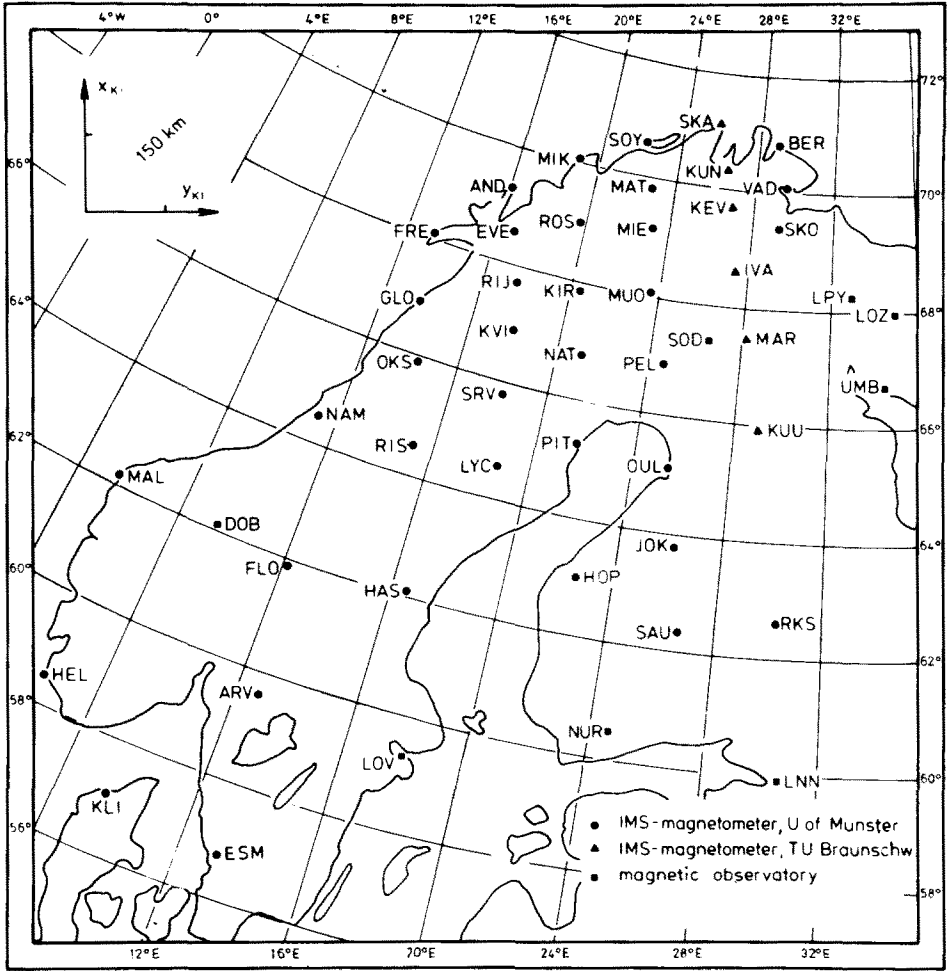


Fig. 1. Station map in geographic co-ordinates of the Münster Gough-Reitzel magnetometers (dots) and the Braunschweig Fluxgate magnetometers (triangles). Also indicated are the axes of the Kiruna cartesian coordinate system.

Analysis

The data from each group were analysed in order to derive estimates of the Inductive Response Function, $C(\omega, k)$ (Schmucker, 1970; Schmucker and Weidelt, 1975) by employing the Horizontal Spatial Gradient (HSG) technique. The response function, $C(\omega, k)$ is defined as the ratio of the vertical magnetic field, $H_z(\omega)$, to the sum of the spatial gradients of the two components of the horizontal magnetic field ($\partial H_x(\omega)/\partial x + \partial H_y(\omega)/\partial y$), i.e.:

$$C(\omega, k) = \frac{H_z(\omega)}{\frac{\partial H_x(\omega)}{\partial x} + \frac{\partial H_y(\omega)}{\partial y}} \quad (1)$$

where k is the Price wavenumber (Price, 1962) of the source field, all at the same frequency ω . For a location where the electrical conductivity of the earth varies with depth alone, $\sigma(z)$, then the Inductive Response Function, $C(\omega, k)$, is directly related to the magnetotelluric impedance, $Z_{xy}(\omega, k)$, by:

$$C(\omega, k) = \frac{1}{i\omega\mu_0} Z_{xy}(\omega, k) \quad (2)$$

Eq. 1 is the basis of the HSG technique, and has been used by Kuckes (1973), Lilley and Sloane (1976), Woods and Lilley (1979), Connerney and Kuckes (1980), Jones (1980), Lilley et al. (1981), and, in a global sense, by Berdichevsky et al. (1976).

To estimate $C(\omega, k)$ for a location from eq. 1, two steps are necessary; (i) deriving, from the synoptic measurements of the magnetic field variations, estimates of the spatial gradient term ($\partial H_x/\partial x + \partial H_y/\partial y$), and (ii) deriving estimated of $C(\omega, k)$. Full details of the methods chosen to accomplish these steps are given in Jones (1980), however, for completeness, the steps are described briefly below.

Step 1

To derive estimates of the spatial gradient terms for each of the three groups, the magnetic time variations, $h_x(t)$, $h_y(t)$, $h_z(t)$, were Fourier transformed into the frequency domain, after suitable preprocessing operations had been carried out, to yield $H_x(\omega)$, $H_y(\omega)$, $H_z(\omega)$. At each Fourier harmonic, ω , the horizontal magnetic field observations in the *KIR* and *KEV* groups were then fitted to second-order 2D polynomial surfaces, such that the curl-free constraint, i.e., $\partial H_x/\partial y = \partial H_y/\partial x$ (no vertical flow of current across the air/earth interface), was upheld. The horizontal field equation consisted of nine unknowns, hence information from a minimum of five stations was required. For the *SAU* group, the horizontal magnetic field variations were fitted to first-order 2D polynomial surfaces, also with the curl-free constraint imposed, of three unknowns. The fit was by least-squares methods which minimised the Euclidean norm between the solutions of the overdetermined system (Golub, 1965).

It is well known that any *local* conductivity inhomogeneities in the crust perturb the vertical magnetic field component, H_z . Hence, direct application of eq. 1 in the vicinity of a lateral variation in electrical conductivity would most likely yield meaningless and uninterpretable estimates of $C(\omega, k)$. The gross area around Kiruna (*KIR*, see Fig. 1) appears to be remarkably free of such inhomogeneities (Jones, 1981a), as does the Sauvamaki (*SAU*, Fig. 1) region (from the small induction vectors observed, fig. 10, Jones, 1981a). However, in order to reduce as much as possible local effects on the observations of H_z , the H_z data in each group were also fitted to 2-degree polynomial surfaces (second-order for *KIR* and *KEV* groups, first-order for *SAU* group), and *regional* mean values of H_z were used.

Step II

Using techniques of statistical frequency analysis, two smoothed estimates of $C(\omega, k)$ were derived. One, $\hat{C}_d(\omega, k)$, was downward biased for any random noise contributions on $(\partial H_x/\partial x + \partial H_y/\partial y)$, the other, $\hat{C}_u(\omega, k)$, was upward biased for any random noise contributions on H_z . The estimate of $C(\omega, k)$ was given by the geometric mean of these two, i.e.:

$$\hat{C}(\omega, k) = \sqrt{\hat{C}_d(\omega, k) \cdot \hat{C}_u(\omega, k)}$$

Response functions derived

Kiruna—KIR

For the Kiruna group of stations, a total of eight events were chosen within which the observed horizontal magnetic field variations were of sufficiently large gradient

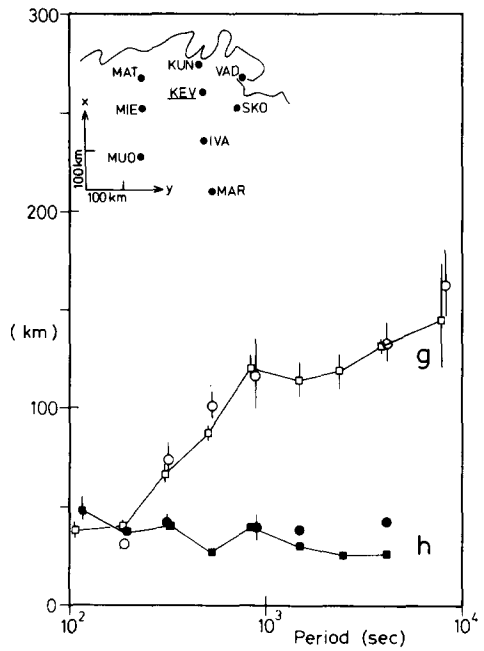
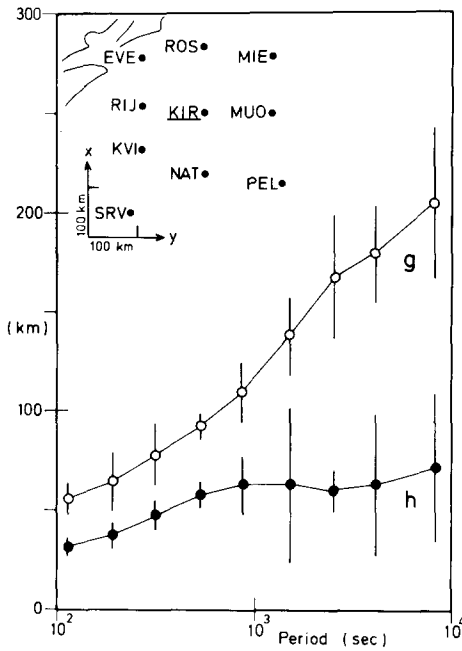


Fig. 2. Estimates of C_{KIR} displayed as \hat{g}_{KIR} (open circles) and \hat{h}_{KIR} (full circles), where $C = g - ih$. The limits are the 95% confidence intervals of the estimates. Also indicated are the stations used in the determination.

Fig. 3. Estimates of C_{KEV} from the two events analysed, displayed as \hat{g}_{KEV} and \hat{h}_{KEV} , where $C = g - ih$. The estimates are: event 1: g —open squares, h —full squares; event 2: g —open circles, h —full circles. The error bars indicate the upward and downward biased estimates, \hat{C}_u and \hat{C}_d . The estimates from event 1, connected together by the full line, were used for further analysis. Also illustrated are the stations used in the determination.

to permit reliable estimation of C_{KIR} . The analysis of these events is described in detail in Jones (1980). Figure 2 illustrates the function \hat{C}_{KIR} , expressed in terms of $\hat{g}_{\text{KIR}}(\omega)$ (open symbols) and $\hat{h}_{\text{KIR}}(\omega)$ (solid symbols) where $C = g - ih$, with their associated 95% confidence intervals.

Kevo—KEV

For the Kevo group, only two events were available which were suitable for analysis. In order to maximise the reliability of the estimates, the “raw” (i.e. unsmoothed) estimates of H_z and of $(\partial H_x/\partial x + \partial H_y/\partial y)$ were subjected to the coherence-based rejection technique proposed by Jones and Jödicke (1982). The resulting improved estimates \hat{C}_{KEV} are illustrated in Fig. 3. The bars indicate the ranges between the downward-biased and the upward-biased estimates. It can be clearly seen in Fig. 3 that the two data sets are totally compatible, and result in similar estimates of C_{KEV} . For further analysis, the more reliable of the two, indicated by open (for \hat{g}_{KEV}) and full (for \hat{h}_{KEV}) squares, was taken.

For locations SKA, KUN, KEV, IVA and MAR (see Fig. 1), there are available three-component magnetic data in the pulsation period band, i.e. 10–600 s, recorded by Göttingen University. Values of \hat{C}_{KEV} were calculated by E. Steveling (pers. commun., 1980) from a simplified form of Eq. 1. These values are illustrated in Fig. 4 at periods of 10 s, 30 s, 90 s, 240 s, and 600 s (open triangles— \hat{g}_{KEV} , solid triangles— \hat{h}_{KEV}), together with the associated error limits. Steveling is of the opinion that the highest (10 s) and lowest (600 s) frequency values are not reliable. It can be seen in Fig. 4 that the remaining estimates are totally in accord with those presented here.

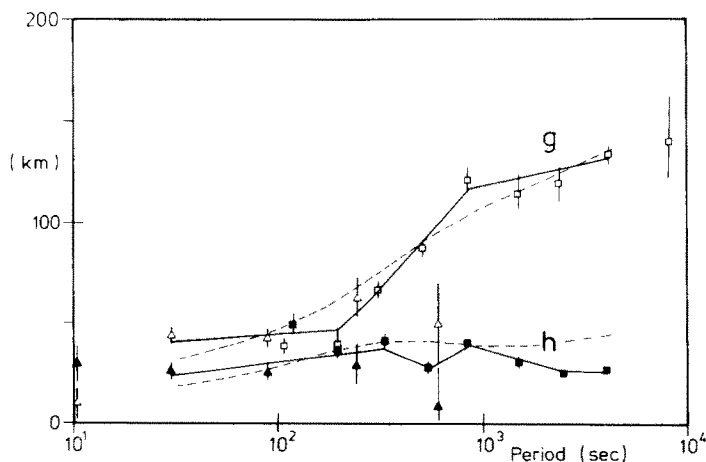


Fig. 4. Estimates of C_{KEV} from event 1 (see Fig. 3) (g —open squares, h —full squares) and from the pulsation data of Steveling (g —open triangles, h —full triangles). The values of \hat{g}_{KEV} and \hat{h}_{KEV} employed in the inversion were derived by interpolating on a logarithmic scale along the full lines illustrated. The dashed line is the best fitting model to the data discovered by the Monte-Carlo random search procedure.

For further analysis, the estimates \hat{g}_{KEV} and \hat{h}_{KEV} were smoothed to the solid lines shown in Fig. 4, and values of \hat{g}_{KEV} and \hat{h}_{KEV} were determined at equal intervals on a logarithmic (period) scale.

Sauvamaki—SAU

For the three stations in the Sauvamaki group, only two events were available, and hence the transfer function improvement technique (Jones and Jödicke, 1982) was applied to these data also. The resulting estimates of C_{SAU} are illustrated in Fig. 5. The estimates \hat{g}_{SAU} are considered to be quite reliable and both data sets display remarkable agreement. The estimates \hat{h}_{SAU} were acceptable from only one of the two data sets analysed.

For Sauvamaki (SAU, see Fig. 1), there are available MT data, consisting of the three-component magnetic data from SAU plus synoptic two-component telluric

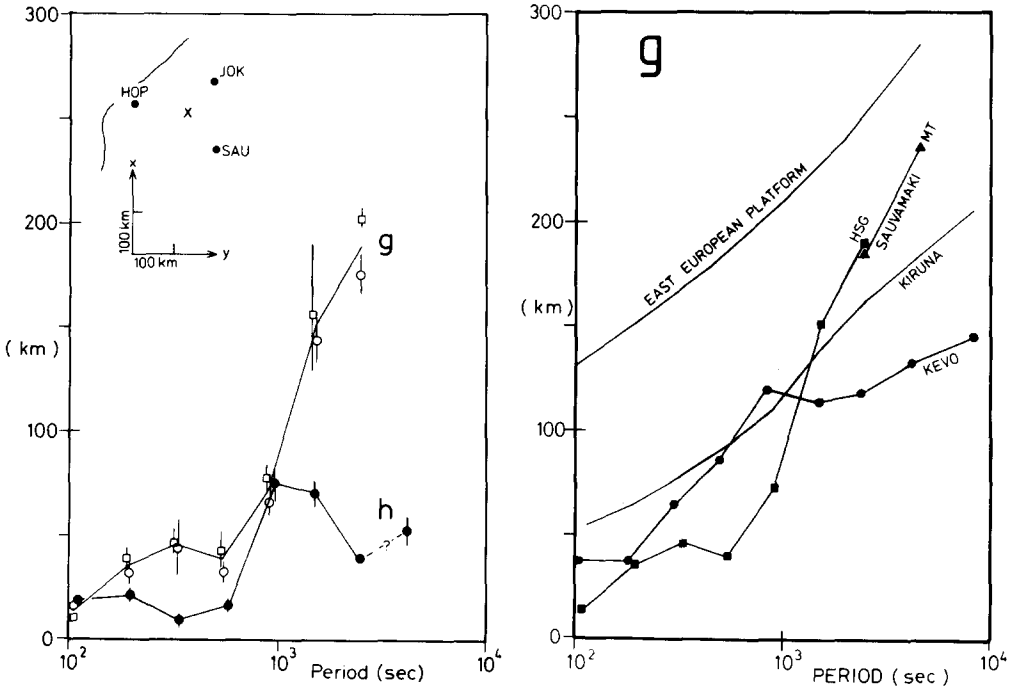


Fig. 5. Estimates of C_{SAU} for the centre of gravity of the three stations employed as indicated by the cross. The estimates are displayed as \hat{g}_{SAU} and \hat{h}_{SAU} , where $C = g - ih$, for event 1 (g —open circles, h —full circles) and event 2 (g —open squares, no “ h ” estimates reliable). The error bars indicate the upward and downward biased estimates, \hat{C}_u and \hat{C}_d . Also illustrated are the stations used in the determination.

Fig. 6. Comparison of the real part of $\hat{C}(\omega)$, i.e., \hat{g} , for the four regions; Kevo—dots; Kiruna—full line; Sauvamaki HSG analysis—squares, Sauvamaki MT analysis—triangles; East European Platform (from Vanyan et al.'s (1977) “generalised” apparent resistivity curve and Weidelt's (1972) approximate phase formula)—full line.

data recorded during July 1979, by the instrumentation reported in Jones et al. (1982). The long period averaged MT impedance values, given by $(\hat{Z}_{xy} - \hat{Z}_{yx})$ (the minus sign accounts for the π phase difference between Z_{xy} and Z_{yx}), expressed as C estimates according to eq. 2, are totally in accord with the long period HSG estimates (see Fig. 6) for \hat{g}_{SAU} .

East European Platform—EEP

In order to be able to compare the derived response functions \hat{C}_{KIR} (Fig. 2), \hat{C}_{KEV} (Figs. 3 and 4), and C_{SAU} (Fig. 5) with what could be expected for a stable Precambrian craton region, the “generalised” apparent resistivity curve for the East European Platform was taken from Vanyan et al. (1977). In the period range 10 – 10^5 s, their data fit approximately to the relationship:

$$\log_{10}(\rho_a(T)) = 4.37 - 0.594 \log_{10}(T) \quad (3)$$

where T is the period of interest, in s, and $\rho_a(T)$ is the apparent resistivity at period T , in ohm \cdot m.

It is relatively well known that the logarithm of apparent resistivity and the phase of the impedance are related, by Hilbert transformation, when the data result from a 1D earth (Weidelt, 1972; Fischer and Schnegg, 1980). Weidelt (1972) has given a formula for deriving the approximate phase compatible with the apparent resistivity data, viz.:

$$\phi(T) \approx \frac{1}{4}\pi \left(1 - \frac{\log(\rho_a(T))}{\log(T)} \right) \quad (4)$$

(eq. 2.28 of Weidelt (1972) refers to the phase of $C(\omega)$). Applying eq. 4 to eq. 3 yields a frequency independent phase in the period range 10 – 10^5 s of $\phi \approx \frac{1}{4}\pi(1 + 0.594)$, i.e., $\phi \approx 0.3985$ radians, or 71.4° . Expressing these apparent resistivity and approximate phase data in terms of $C(\omega, 0)$, using eq. 2, yields $g_{EEP}(\omega)$ as illustrated in Fig. 6.

Validity of interpretation of $C(\omega, 0)$

Eq. 1 is an expression for determining $C(\omega, k)$ from knowledge of $H_z(\omega)$ and $(\partial H_x(\omega)/\partial x + \partial H_y(\omega)/\partial y)$. In order to be able to interpret the observed responses, it appears as-if knowledge of the relevant source wavenumber, k , for the particular event analysed is a prerequisite. However, Berdichevsky et al. (1981) have shown recently that the expression in $C(\omega, k)$ can be expanded in terms of $C(\omega, 0)$ employing odd-order derivatives of the horizontal field spatial gradient, viz.:

$$\begin{aligned} H_z(\omega) &= C(\omega, k) \left(\frac{\partial H_x(\omega)}{\partial x} + \frac{\partial H_y(\omega)}{\partial y} \right) \\ &= C(\omega, 0) \left(\frac{\partial H_x(\omega)}{\partial x} + \frac{\partial H_y(\omega)}{\partial y} \right) + \frac{I_2}{2!} \left(\frac{\partial^3 H_x(\omega)}{\partial x^3} + \frac{\partial^3 H_y(\omega)}{\partial y^3} \right) + \dots \quad (5) \end{aligned}$$

In the functional representation of the horizontal fields ($H_x(\omega)$, $H_y(\omega)$), only first- or second-order polynomials were fitted to the observations. Hence third- and higher-order derivatives of the spatial gradient were minimised in the least-squares fit, with the result that the derived functions are for $k = 0$, i.e., uniform source field, and may be interpreted as such. Henceforth $C(\omega)$ refers to $C(\omega, 0)$.

In the following section, \hat{C}_{KIR} and \hat{C}_{KEV} will be interpreted in terms of 1D models, i.e., in which conductivity is a function of depth alone. No *sufficient* conditions on $C(\omega)$ to permit such an interpretation have as yet been derived, but Weidelt (1972) details nine *necessary* conditions on $C(\omega)$. Writing $C(\omega)$ in terms of its real and imaginary parts as $C = g - ih$, and defining operator D as $Df =$

TABLE I

Application of Weidelt's inequality conditions on the estimated functions C_{KIR} , C_{KEV} , and C_{SAU} (see text and eqs. 6.1–6.9). + indicates inequality was upheld; – indicates inequality was violated

Location	Period (s)	Test								
		6.1	6.2	6.3	6.4	6.5	6.6	6.7	6.8	6.9
Kir	115.0	+	+	+	+	+	+	+	+	+
	190.0	+	+	+	+	+	+	+	+	+
	320.0	+	+	+	+	+	+	+	+	+
	535.0	+	+	+	+	+	+	+	+	+
	890.0	+	+	+	+	+	+	+	+	+
	1490.0	+	+	+	+	+	+	+	+	+
	2480.0	+	+	+	+	+	+	+	+	+
	4090.0	+	+	+	+	+	+	+	+	+
	8200.0	+	+	+	+	+	+	+	+	+
KEV	33.0	+	+	+	+	+	+	+	+	+
	55.0	+	+	+	+	+	+	–	+	+
	100.0	+	+	+	+	+	+	–	+	–
	175.0	+	+	+	+	+	+	+	+	–
	333.0	+	+	+	+	+	–	+	+	+
	555.0	+	+	+	+	+	–	+	+	+
	1000.0	+	+	+	+	+	+	+	+	+
	1750.0	+	+	+	+	+	+	+	+	+
	3333.0	+	+	+	+	+	+	+	+	+
SAU	115.0	+/+	+/+	+/+	+/+	-/+	-/-	-/-	-/-	-/-
	200.0	+/+	+/+	+/+	+/+	+/+	-/-	-/+	-/+	-/-
	320.0	+/+	+/+	+/+	+/+	+/+	-/-	+/+	-/-	-/-
	540.0	+/+	+/+	+/+	+/+	-/+	-/-	-/+	-/-	-/+
	900.0	+/+	+/+	+/+	+/+	-/+	-/-	+/+	-/-	-/-
	1500.0	+/+	+/+	+/+	+/+	+/+	-/-	+/+	-/-	+/+
	2500.0	+/+	+/+	+/+	+/+	+/+	-/-	-/+	-/-	+/+

(Signs before the slash are the original data, signs after the slash refer to the Hanning smoothed data.)

– $df/d(\log T)$, these conditions are:

$$g \geq 0, \quad h \geq 0 \quad (6.1, 6.2)$$

$$Dg \geq 0 \quad (6.3)$$

$$0 \leq -D|C| \leq |C| \quad (6.4, 6.5)$$

$$|DC| \leq h, \quad |C + DC| \leq g \quad (6.6, 6.7)$$

$$|D^2C| \leq h, \quad |C + 2DC + D^2C| \leq g \quad (6.8, 6.9)$$

The physical interpretation of conditions (6.1) and (6.2) is that the phase lead of the electric (telluric) field over the magnetic field must lie between 0° – 90° . Condition (6.3) is the skin-effect requirement; the longer the period of observation, the deeper within the earth must flow the induced eddy currents. The depth of maximum eddy current flow, or the depth of the “centre of gravity” of the in-phase induced current system, is given by g (Weidelt, 1972).

Applying these conditions as tests on the response functions \hat{C}_{KIR} and \hat{C}_{KEV} illustrate that \hat{C}_{KIR} is totally consistent with a 1D earth, and \hat{C}_{KEV} almost totally consistent (see Table I). However, the original estimates \hat{C}_{SAU} violated 26 of the 63 inequalities (i.e., nine inequalities applied at seven frequencies). Smoothing the estimates \hat{C}_{SAU} by a Hanning window, i.e., $(\frac{1}{4}, \frac{1}{2}, \frac{1}{4})$, resulted in an increased number of upheld inequalities, but eighteen of the 63 were still violated (Table I). Hence \hat{C}_{SAU} was not considered reliably enough estimated to justify sophisticated 1D inversion (see following section), because of \hat{h}_{SAU} , and only \hat{g}_{SAU} is used further. That \hat{g}_{SAU} is well estimated was shown by comparison with recent analysis of MT data recorded at Sauvamäki (SAU, see Fig. 1) by Jones et al. (1982).

MODELS CONSISTENT WITH THE OBSERVATIONS

Having derived the response functions \hat{C}_{KIR} and \hat{C}_{KEV} , many inversion methods exist for deriving 1D earth models consistent with the observations. A first-approximation is given by the $\rho^* - z^*$ inversion of Schmucker (1970). Resistivity ρ^* is a first approximation to the true resistivity at a depth of z^* . The terms ρ^* and z^* are given from the inductive response function $C(\omega)$, by

$$\rho^*(z^*) = 2\omega\mu_0 h^2, \quad z^* = g \quad (7.1, 7.2)$$

For the functions \hat{C}_{KIR} , \hat{C}_{KEV} , and C_{EEP} , the $\rho^* - z^*$ inversions are illustrated in Fig. 7, where a great difference can be seen between the three regions.

The response \hat{C}_{KIR} has been inverted elsewhere (Jones, 1982), and the resulting best-fitting model discovered consistent with the observations is illustrated in Fig. 9. The data were inverted by a Monte-Carlo random search procedure (Jones and Hutton, 1979), with the constraints imposed that the acceptable solutions all had a top layer of 10^4 ohm · m (from the audio-magnetotelluric work of Westerlund, 1972), and that the depth to the second interface for all solutions was 46 km (present best

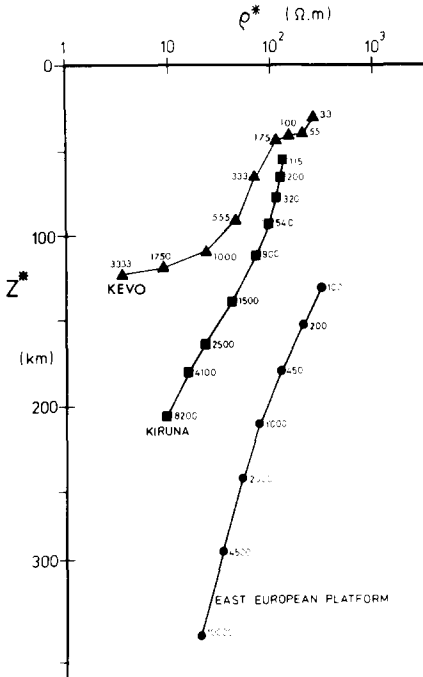


Fig. 7. Schmucker ρ^*-z^* inversion of response functions \hat{C}_{KEV} , \hat{C}_{KIR} , and C_{EEP} . The numbers are the period of interest.

estimate of the Moho depth in central northern Sweden (Bungum et al., 1980)). The upper crustal layer, assumed here to be of 10^4 ohm \cdot m, is virtually invisible at the periods of 10^2 s, but its existence is important for correct determination of the parameters of the underlying layers. Any value in the range 10^3 to 10^5 ohm \cdot m would be acceptable. That the data could resolve the parameters of the final model, with the exception of the top layer resistivity, was shown by application of certain aspects of Generalized Linear Inversion theory to the problem (Jones, 1982).

For the inversion by the Monte-Carlo procedure of \hat{C}_{KEV} , it seems reasonable to assume: (i) that the upper mantle beneath northern Finland will have a similar conductivity to that under northern Sweden, (ii) that the Moho interface be again at 46 km (Bungum et al., 1980), and (iii) that the resistivity of the electrical asthenosphere be in the range 1–10 ohm \cdot m, which is consistent with other observations (Cox et al., 1980; Oldenburg, 1981; Filloux, 1981) and with the value derived for the high conducting zone under northern Sweden. Accordingly, the model parameters were constrained such that four-layer models were randomly chosen from the seven-dimensional parameter space with the fixed requirements that $d_2 = 46$ km, $\rho_3 = 80$ ohm \cdot m, and $\rho_4 = 5$ ohm \cdot m. The models accepted, from 6000 randomly chosen, had $\rho-d$ profiles as illustrated in Fig. 8. It is apparent from the figure that

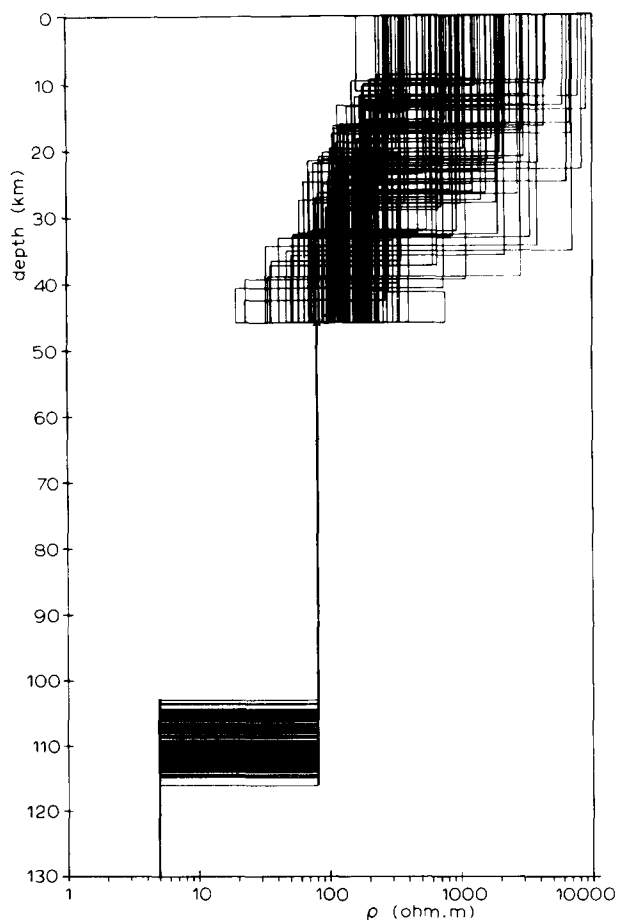


Fig. 8. Monte-Carlo inversion of \hat{C}_{KEV} illustrating acceptable models in terms of their ρ - d profiles. The model search was constrained to discover permissible solutions with parameters d_2 , ρ_3 , ρ_4 , set to the values; $d_2=46$ km (depth to Moho (Bungum et al., 1980)), $\rho_3=80$ ohm·m (consistency with Kiruna upper mantle resistivity (Jones, 1982)), $\rho_4=5$ ohm·m (asthenospheric resistivity as determined by various studies (see text)).

the crustal layers are not well delineated, and the parameters ρ_1 , d_1 and ρ_2 can take any values in the ranges:

$$\rho_1 = 200-10^4 \text{ ohm} \cdot \text{m}, \quad d_1 = 9-42 \text{ km}, \quad \rho_2 = 20-400 \text{ ohm} \cdot \text{m}$$

The most probable value, as given by ± 1 standard deviation from the mean, for ρ_2 is in the range 100–300 ohm·m, which is exactly the same resistivity as that deduced for the lower crustal layer beneath central northern Sweden. This resistivity for a lower crustal layer beneath a Precambrian region classifies it as Type II according to the classification system proposed by Jones (1981b). It is most likely that anhydrous

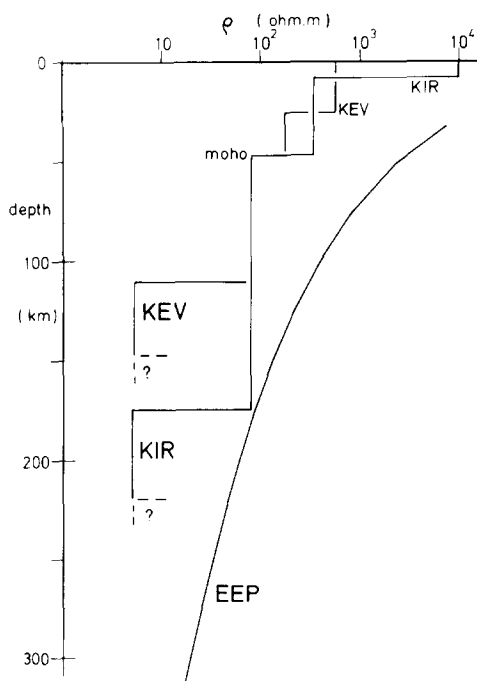


Fig. 9. Models for the regions of (i) northern Sweden (Kiruna), (ii) northern Finland/northeastern Norway (Kevo), and (iii) East European Platform (Vanyan, 1981).

conditions exist in the lower crust to explain these moderate resistivities (Jones, 1981b), and a rock type consistent with the characteristics displayed of the Type II class is an amphibolite. (It is expected that a seismic study in northern Finland would determine that the lower crust displayed a compressional wave velocity of around $V_p \approx 7.0$ km/s.) The Monte-Carlo procedure describes well that there must be a transition to a good conducting zone between 103–115 km in order to explain the observed response function \hat{C}_{KEV} . The best-fitting model to the data is shown by its ρ - d profile in Fig. 9 and its theoretical response is illustrated in Fig. 4 (dashed line). No attempt was made to try to reproduce the local minimum in h_{SAU} at 500 s. That the theoretical and observed values of h_{SAU} begin to diverge at the longest periods may be due to the finite thickness of the asthenosphere.

For the East European Platform, Vanyan (1981) has presented a ρ - d profile, believed by him to be normal for a cratonic region (Fig. 9). This profile is characterised by a monotonically increasing conductivity with depth, and the absence of any conducting zone in the depth range 80–250 km.

IMPLICATIONS TO THE ASTHENOSPHERE BELOW SCANDINAVIA

General comments

The good conducting layer, which must exist at around 110 km depth beneath northern Finland/northeastern Norway, and around 170 km depth beneath northern Sweden, in order to satisfy the observed responses \hat{C}_{KEV} and \hat{C}_{KIR} respectively, appears to have an electrical resistivity in the range 1–10 ohm · m. Such a value is consistent with other observations of conducting zones in the Earth's upper mantle at depths of the order of 80–200 km defined by electromagnetic induction studies undertaken in the Atlantic (Cox et al., 1980) and the Pacific (Filloux, 1980, 1981; Oldenburg, 1981) oceans. In the latter case of the Pacific ocean, a strong correlation was discovered between the age of the oceanic crust and the depth to the good conducting layer for the three sites investigated. The respective ages, depths to the maximum in electrical conductivity, and values of electrical resistivity at those depths, for the locations were: 1 Ma, 60 km, 5 ohm · m; 30 Ma, 130 km, 5 ohm · m; 72 Ma, 180 km, 20 ohm · m, i.e., the depth to the electrical asthenosphere increases with increasing distance from the mid-oceanic trench.

It is reasonable to assume that this situation is also true of the mid-Atlantic ridge, in particular the Reykjanes spreading centre with the deepening asthenosphere with distance towards the Norwegian coast. At a non-tectonic ocean–continent margin such as the eastern Atlantic, there will not be an abrupt change in the asthenosphere, rather a gradual deepening of the asthenospheric layer with distance into the continent. Kiruna (KIR, see Fig. 1) lies some 250 km from the continental edge (see bathymetry map, fig. 12, Jones, 1981a), and hence an asthenosphere beneath Kiruna at a depth of around 170 km is reasonable. Seismic observations have also inferred a low compressional wave velocity zone, LV_pL , beneath Sweden at a depth of between 170–190 km (Cassell and Fuchs, 1979), 150–250 km (Nolet, 1977), and 150–220 km (Given and Helmberger, 1980). The electrical asthenosphere begins around 170 km, and must be at least 40 km thick or its base would be observed in the response function \hat{C}_{KIR} .

Further toward the centre of the East European Platform, there is the inference from \hat{g}_{SAU} (Fig. 6) that beneath SAU the depth to the conducting zone is of the order of 210 km (taken from the value of \hat{g}_{SAU} at a period of 3000 s, which is the period at which \hat{g}_{KIR} and \hat{g}_{KEV} infer the depth to their conducting zones). For the East European Platform itself, and for the Karelian megablock of the Baltic shield (Kaikkonen et al., 1981), the depth to the 10 ohm · m zone in the upper mantle is > 300 km.

One result from this study of startling importance is that the electrical asthenosphere beneath northern Finland/northeastern Norway begins at a depth of around 110 km (Fig. 8). This zone must also be at least 40 km thick. Such a shallow asthenosphere is somewhat unexpected considering that the Barents Sea is of less

than 500 m depth over its whole extent, i.e., not a true “ocean” in the plate tectonic sense. Certainly seismic work undertaken in the Barents Sea may yield some very interesting results with regard to the lithosphere and asthenosphere. The enhancement of the vertical magnetic field component, H_z , at the northern Norwegian coast has already been noted as anomalously large by Jones (1981a).

Inferred temperature of the asthenosphere

As discussed in the previous section, the conductivity of the zone defined as the electrical asthenosphere appears to lie in the range 0.1–1.0 S/m. The possible inferences as to the temperature of the asthenosphere rests with the decision of whether the dominant conduction mechanism is ionic or electrolytic, and if electrolytic, what the likely electrolyte is.

For an ionic conduction mechanism in dry rock, the work of Duba et al. (1974) and Shankland and Waff (1977) on olivine, which is believed to be a good approximation to the composition of the upper mantle (Birch, 1970), suggest temperatures in excess of 1600°C to explain a conductivity value as low as 0.2 S/m. Such temperatures are certainly far too high for a convective heat transfer model of the mantle. Rai and Manghnani's (1978) studies on solid ultramafic rocks infer temperatures of 1150°C and 1300°C for garnet lherzolite and spinel lherzolite respectively, which are their lower and upper bounds for all the various rocks they investigated.

The existence of the seismic low compressional wave velocity layer (LV_pL) beneath Sweden is believed to require a 1–3% melt fraction of the rock to provide the required reduced seismic velocities (see, for example, Stocker and Gordon, 1975). A 2% melt fraction at a pressure of 50 kbar with an effective conductivity of 0.2 S/m infers a temperature around 1500°C from the effective medium theory of Shankland and Waff (1977) as applied to a basalt/olivine mix. Hence, it appears that a value of around 1500°C may be taken as the maximum upper bound on any possible temperature of the asthenosphere.

Tozer (1981) is of the opinion, however, that the rôle of meteoric water contained in cracks and pores is extremely important. For a water concentration of $\sim 10^{-4}$ (which is believed by Tozer (1981) to be the limit beyond which diapirism initiates and balances the water budget between subducting oceanic water and magmatic loss), a bulk conductivity of 0.2 S/m, and assuming a very idealised model of the permeable material, a network material electrical conductivity of $\sim 10^4$ is inferred. Such a value implies, for a saturated aqueous solution, a temperature of $\sim 900^\circ\text{C}$ (see Tozer, 1981, for details). It is certainly true that should there be water present in significant quantities in the asthenosphere, then the dry rock temperatures are all well above Kushiro et al.'s (1968) hydrous lherzolite solidus, which is around 1000–1100°C at depths of 100–200 km.

In conclusion therefore, it appears that a whole range of temperatures, from 900

to 1500°C, may be, by suitable choice of environmental parameters, consistent with the observed electrical conductivity value for the asthenosphere. Until more is known of the prevailing conditions within the asthenosphere (water content, melt fraction, etc), speculation as to the probable temperature of the asthenosphere from geomagnetic induction data appears to be a somewhat academic exercise.

ACKNOWLEDGEMENTS

The author wishes to acknowledge the support of the Deutsche Forschungsgemeinschaft during his stay at Münster. He is also very grateful to E. Steveling (Göttingen) for providing the short period \hat{C}_{KEV} estimates, and to H. Maurer (Braunschweig) for providing his magnetic data from stations SKA, KUN, KEV, IVA, and MAR.

This manuscript was completed whilst the author was at the Swedish Geological Survey (SGU, Uppsala).

REFERENCES

- Berdichevsky, M.N., Fainberg, E.B., Rotanova, N.M., Smirnov, J.B. and Vanyan, L.L., 1976. Deep electromagnetic investigations. *Ann. Geophys.*, 32: 143–155.
- Berdichevsky, M.N., Dmitriev, V.I. and Schmucker, U., 1981. Generalised magnetotelluric and magnetic gradient relation for a layered half-space. Paper presented at 4th IAGA Scientific Assembly, Edinburgh, August 3–15, mimeographed.
- Birch, F., 1970. Density and composition of the upper mantle: first approximation as an olivine layer. In: *The Earth's Crust and Upper Mantle*. Am. Geophys. Union, Monogr., 13: 18–36.
- Bungum, H., Pirhonen, S.E. and Husebye, E.S., 1980. Crustal thickness in Fennoscandia. *Geophys. J.R. Astron. Soc.*, 63: 759–774.
- Cassell, B.R. and Fuchs, K., 1979. Seismic investigations of the subcrustal lithosphere beneath Fennoscandia. *J. Geophys.*, 46: 369–384.
- Connerney, J.E.P. and Kuckes, A.F., 1980. Gradient analysis of geomagnetic fluctuations in the Adirondacks. *J. Geophys. Res.*, 85: 2615–2624.
- Cox, C.S., Filloux, J.H., Gough, D.I., Larsen, J.C., Poehls, K.A., Von Herzen, R.P. and Winter, R., 1980. Atlantic lithospheric sounding. In: *Electromagnetic Induction in the Earth and Moon*, AEPS-9. Centr. Acad. Publ. Japan, Tokio, and D. Reidel Publ. Co., Dordrecht, U. Schmucker (Editor), Suppl. Issue J. Geomagn. Geoelectr., pp. 13–32.
- Duba, A.G., Heard, H.C. and Schock, R.N., 1974. Electrical conductivity of olivine at high pressures and under controlled oxygen fugacity. *J. Geophys. Res.*, 79: 1667–1673.
- Filloux, J.H., 1980. North Pacific magnetotelluric experiments. In: *Electromagnetic Induction in the Earth and Moon*, AEPS-9. Centr. Acad. Publ. Japan, Tokio, and D. Reidel Publ. Co., Dordrecht, U. Schmucker (Editor), Suppl. Issue J. Geomagn. Geoelectr., pp. 33–43.
- Filloux, J.H., 1981. Magnetotelluric exploration of the North Pacific: progress report and preliminary soundings near a spreading ridge. *Phys. Earth Planet. Inter.*, 25: 187–195.
- Fischer, G. and Schnegg, P.-A., 1980. The dispersion relations of the magnetotelluric response and their incidence on the inversion problem. *Geophys. J.R. Astron. Soc.*, 62: 661–673.
- Frazer, M.C., 1974. Geomagnetic sounding with arrays of magnetometers. *Rev. Geophys. Space Phys.*, 12: 401–420.

- Given, J.W. and Helmsberger, D.V., 1980. Upper mantle structure of northwestern Europe. *J. Geophys. Res.*, 85: 7183–7194.
- Golub, G., 1965. Numerical methods for solving linear least-squares problems. *Numer. Math.*, 7: 206–216.
- Gough, D.I., 1973a. The interpretation of magnetometer array studies. *Geophys. J. R. Astron. Soc.*, 35: 85–98.
- Gough, D.I., 1973b. The geophysical significance of geomagnetic variation anomalies. *Phys. Earth Planet. Inter.*, 7: 379–388.
- Gough, D.I. and Reitzel, J.S., 1967. A portable three component magnetic variometer. *J. Geomagn. Geoelectr.*, 19: 203–215.
- Jones, A.G., 1980. Geomagnetic induction studies in Scandinavia—I. Determination of the Inductive Response Function from the magnetometer array data. *J. Geophys.*, 48: 181–194.
- Jones, A.G., 1981a. Geomagnetic induction studies in Scandinavia—II. Geomagnetic depth sounding, induction vectors and coast-effect. *J. Geophys.*, 50: 23–36.
- Jones, A.G., 1981b. On a type classification of lower crustal layers under Precambrian regions. *J. Geophys.*, 49: 226–233.
- Jones, A.G., 1982. On the electrical crust–mantle structure in Fennoscandia: No Moho, and the Asthenosphere revealed? *Geophys. J. R. Astron. Soc.*, 68: 371–388.
- Jones, A.G. and Hutton, R., 1979. A multi-station magnetotelluric study in southern Scotland—II. Monte-Carlo inversion of the data and its geophysical and tectonic implications. *Geophys. J. R. Astron. Soc.*, 56, 351–368.
- Jones, A.G. and Jödicke, H., 1982. Improved response function estimation by a coherence based rejection technique, with special application to magnetotelluric data. *Geophysics*, submitted.
- Jones, A.G., Olafsdottir, B. and Tiikkainen, J., 1982. Geomagnetic induction studies in Scandinavia—III. Magnetotelluric observations. *J. Geophysics*, submitted.
- Kaikkonen, P., Hjelt, S.-E., Pajumpää, K., Vanyan, L.L., Osipova, I.L. and Shilovski, P.P., 1981. A preliminary geoelectric model of the Karelian megablock of the Baltic shield. Paper presented at 4th IAGA Scientific Assembly, Edinburgh, August 3–15, mimeographed.
- Kuckes, A.F., 1973. Relations between electrical conductivity of a mantle and fluctuating magnetic fields. *Geophys. J. R. Astron. Soc.*, 32: 119–131.
- Küppers, F. and Post, H., 1981. A second generation Gough–Reitzel magnetometer. *J. Geomagn. Geoelectr.*, 33: 225–237.
- Küppers, F., Untiedt, J., Baumjohann, W., Lange, K. and Jones, A.G., 1979. A two-dimensional magnetometer array for ground-based observations of auroral zone electric currents during the International Magnetospheric Study (IMS). *J. Geophys.*, 46: 429–450.
- Kushiro, I., Syono, Y. and Akimoto, S.-I., 1968. Melting of a peridotite nodule at high pressures and high water pressures. *J. Geophys. Res.*, 73: 6023–6029.
- Lilley, F.E.M., 1975. Magnetometer array studies: A review of the interpretation of observed fields. *Phys. Earth Planet. Inter.*, 10: 231–240.
- Lilley, F.E.M. and Sloane, M.N., 1976. On estimating electrical conductivity using gradient data from magnetometer arrays. *J. Geomagn. Geoelectr.*, 28: 321–328.
- Lilley, F.E.M., Woods, D.V. and Sloane, M.N., 1981. Electrical conductivity from Australian magnetometer arrays using spatial gradient data. *Phys. Earth Planet. Inter.*, 25: 202–209.
- Maurer, H. and Theile, B., 1978. Parameters of the auroral electrojet from magnetic variations along a meridian. *J. Geophys.*, 44: 415–426.
- Nolet, G., 1977. The upper mantle under western Europe inferred from the dispersion of Rayleigh modes. *J. Geophys.*, 43: 265–285.
- Oldenburg, D.W., 1981. Conductivity structure of oceanic upper mantle beneath the Pacific Plate. *Geophys. J. R. Astron. Soc.*, 65: 359–394.

- Price, A.T., 1962. The theory of magnetotelluric fields when the source field is considered. *J. Geophys. Res.*, 67: 1907–1918.
- Rai, C.S. and Manghnani, M.H., 1978. The effects of saturant salinity and pressure on the electrical resistivity of Hawaiian basalts. *Geophys. J. R. Astron. Soc.*, 65: 395–405.
- Schmucker, U., 1970. Anomalies of geomagnetic variations in the southwestern United States. *Bull. Scripps Inst. Oceanogr.*, 13 Univ. California Press,
- Schmucker, U. and Weidelt, P., 1975. Electromagnetic induction in the Earth. Lecture Notes, Aarhus University, Aarhus, mimeographed.
- Shankland, T.J. and Waff, H.S., 1977. Partial melting and electrical conductivity anomalies in the upper mantle. *J. Geophys. Res.*, 82: 5409–5417.
- Stocker, R.L. and Gordon, R.B., 1975. Velocity and internal friction in partial melts. *J. Geophys. Res.*, 80: 4828–4836.
- Tozer, D.C., 1981. The mechanical and electrical properties of Earth's asthenosphere. *Phys. Earth Planet. Inter.*, 25: 280–296.
- Vanyan, L.L., 1981. Deep geoelectrical models: geological and electromagnetic parameters. *Phys. Earth Planet. Inter.*, 25: 273–279.
- Vanyan, L.L., Berdichevsky, M.N., Fainberg, E.B. and Fiskina, M.V., 1977. The study of the asthenosphere of the East European Platform by electromagnetic sounding. *Phys. Earth Planet. Inter.*, 14: P1–P2 (Letter Section).
- Weidelt, P., 1972. The inversion problem of geomagnetic induction. *J. Geophys.*, 38: 257–289.
- Westerlund, S., 1972. Magnetotelluric experiments in the frequency range 0.01 Hz to 10 kHz. *KGO Rep.* 72: 10, Kiruna Geophys. Observatory, November.
- Woods, D.V. and Lilley, F.E.M., 1979. Geomagnetic induction in central Australia. *J. Geomagn. Geoelectr.*, 31: 449–458.